Charge Noise Spectroscopy Using Coherent Exchange Oscillations in a Singlet-Triplet Qubit

O. E. Dial,[1] M. D. Shulman,[1] S. P. Harvey,[1] H. Bluhm,[1,*] V. Umansky,[2] and A. Yacoby[1]

[1]*Department of Physics, Harvard University, Cambridge, Massachusetts 02138, USA*

[2]*Department of Condensed Matter Physics, Braun Center for Submicron Research, Weizmann Institute of Science, Rehovot 76100, Israel*

(Received 23 October 2012; published 5 April 2013)

Two level systems that can be reliably controlled and measured hold promise as qubits both for metrology and for quantum information science. Since a fluctuating environment limits the performance of qubits in both capacities, understanding environmental coupling and dynamics is key to improving qubit performance. We show measurements of the level splitting and dephasing due to the voltage noise of a GaAs singlet-triplet qubit during exchange oscillations. Unexpectedly, the voltage fluctuations are non-Markovian even at high frequencies and exhibit a strong temperature dependence. This finding has impacts beyond singlet-triplet qubits since nearly all solid state qubits suffer from some kind of charge noise. The magnitude of the fluctuations allows the qubit to be used as a charge sensor with a sensitivity of $2 \times 10^{-8} e/\sqrt{\mathrm{Hz}}$, 2 orders of magnitude better than a quantum-limited rf single electron transistor. Based on these measurements, we provide recommendations for improving qubit coherence, allowing for higher fidelity operations and improved charge sensitivity.

DOI: 10.1103/PhysRevLett.110.146804 PACS numbers: 85.35.Be, 03.67.−a, 07.50.Ls, 76.60.Lz

Two level quantum systems (qubits) are emerging as promising candidates both for quantum information science [1] and for sensitive metrology [2,3]. When prepared in a superposition of two states and allowed to evolve, the qubit precesses with a frequency proportional to the splitting between the levels. However, on a time scale of the coherence time T_2, the qubit loses its quantum information due to interactions with its noisy environment. This causes qubit oscillations to decay and limits the fidelity of quantum control and the precision of qubit-based measurements. In this work, we study singlet-triplet (S-T_0) qubits, a particular realization of spin qubits [4–17] similar to that in Ref. [18].

Previous work on S-T_0 qubits focused on x (ΔB_Z) rotations, which are dephased by fluctuations in the nuclear bath [19–21]. Here, we focus on the exchange interaction, which creates a splitting J between the $|S\rangle$ and $|T_0\rangle$ states when the (1, 1) and (0, 2) $|S\rangle$ states of the double quantum dot are brought near resonance [Fig. 1(c)]. The value of J depends on the energy detuning between the quantum dots ϵ. The exchange interaction drives single- and two-qubit operations in S-T_0, single-spin, and exchange-only qubits [5,18,22–27]. Exchange oscillations are dephased by fluctuations in J [Fig. 1(c)] driven, for example, by ϵ (voltage) fluctuations between the dots with a tunable sensitivity proportional to $dJ/d\epsilon$ [Fig. 1(d)] [28]. We show that this controllable sensitivity is a useful experimental tool for probing the noise bath dynamics. Previous studies have shown the decay of exchange oscillations within a few π rotations [22,29], but a detailed study of the nature of the noise bath giving rise to this decay is still lacking. In this work, using nuclear feedback to control x rotations [30], we systematically explore the low-frequency noise portion of the voltage noise bath, introduce a new Hahn-echo-based measurement of the high-frequency components of the noise bath, and probe the temperature dependence of both portions. We note that, for all experiments described in this work, the proximal charge sensor used to read the state of the qubit is only biased during measuring, assuring that the charge sensor does not contribute to qubit dephasing (see the Supplemental Material [31]).

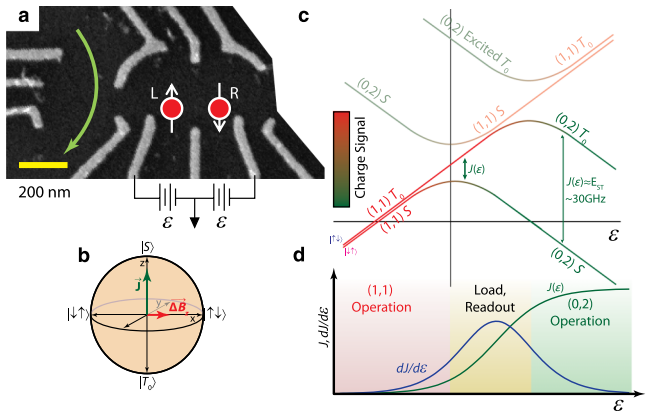

FIG. 1 (color online). (a) The device used in these measurements is a gate-defined S-T_0 qubit with an integrated rf sensing dot. (b) The Bloch sphere that describes the logical subspace features two rotation axes (J and ΔB_Z) controlled with dc voltage pulses. (c) An energy diagram of the relevant states as a function of ϵ. States outside of the logical subspace of the qubit are grayed out. (d) $J(\epsilon)$ and $dJ/d\epsilon$ in three regions: the (1, 1) region where J and $dJ/d\epsilon$ are both small and S-T_0 qubits are typically operated, the transitional region where J and $dJ/d\epsilon$ are both large where the qubit is loaded and measured, and the (0, 2) region where J is large but $dJ/d\epsilon$ is small and large quality oscillations are possible.

The simplest probe of J and its fluctuations is a free induction decay (FID) experiment, in which the qubit is allowed to freely precess for a time t under the influence of the exchange splitting. For FID measurements, we use a $\pi/2$ pulse around the x axis to prepare and read out the state of the qubit along the y axis [Fig. 2(a) and Fig. S1]. Figure 2(b) shows qubit oscillations as a function of t for many different values of ϵ. By measuring the period of these oscillations, we extract $J(\epsilon)$ and we calculate $dJ/d\epsilon$ by fitting $J(\epsilon)$ to a smooth function and differentiating [Fig. 2(c)]. For negative ϵ (small J), we empirically find across many devices and tunings that J is well described by $J(\epsilon) \simeq J_0 + J_1 \exp(\epsilon/\epsilon_0)$.

The oscillations in these FID experiments decay due to voltage noise from dc up to a frequency of approximately $1/t$. As the relaxation time T_1 is in excess of 100 μs in this regime, T_1 decay is not an important source of decoherence (Fig. S4). The shape of the decay envelope and the scaling of coherence time with $dJ/d\epsilon$ (which effectively changes the magnitude of the noise) reveal information about the underlying noise spectrum. White (Markovian) noise, for example, results in an exponential decay of e^{-t/T_2^*}, where $T_2^* \propto (dJ/d\epsilon)^{-2}$ is the inhomogeneously broadened coherence time [32]. However, we find that the decay is Gaussian [Fig. 2(d)] and that T_2^* [black line in Fig. 2(e)] is proportional to $(dJ/d\epsilon)^{-1}$ [solid red line in Fig. 2(e)] across 2 orders of magnitude of T_2^*. Both of these findings can be explained by quasistatic noise, which is low frequency compared to $1/T_2^*$. In such a case, one expects an amplitude decay of the form $\exp[-(t/T_2^*)^2]$, where $T_2^* = \frac{1}{\sqrt{2}\pi(dJ/d\epsilon)\epsilon_{\rm rms}}$ and $\epsilon_{\rm rms}$ is the root-mean-squared fluctuation in ϵ (Eq. S3). From the ratio of T_2^* to $(dJ/d\epsilon)^{-1}$, we calculate $\epsilon_{\rm rms} = 8$ μV in our device. At very negative ϵ, J becomes smaller than ΔB_z, and nuclear noise limits T_2^* to approximately 90 ns, which is consistent with previous work [30]. We confirm that this effect explains deviations of T_2^* from $(dJ/d\epsilon)^{-1}$ by using a model that includes the independently measured $T_{2,\rm nuclear}^*$ and ΔB_z (Eq. S1) and observe that it agrees well with measured T_2^* at large negative ϵ [dashed red line in Fig. 2(e)].

Since we observe J to be approximately an exponential function of ϵ ($dJ/d\epsilon \sim J$) we expect and observe the quality (number of coherent oscillations) of these FID oscillations $Q \equiv JT_2^*/2\pi \sim J(dJ/d\epsilon)^{-1}$ to be approximately constant regardless of ϵ. However, when ϵ is made very positive and J is large, an avoided crossing occurs between the (1, 1) $|T_0\rangle$ and the (0, 2) $|T_0\rangle$ states,

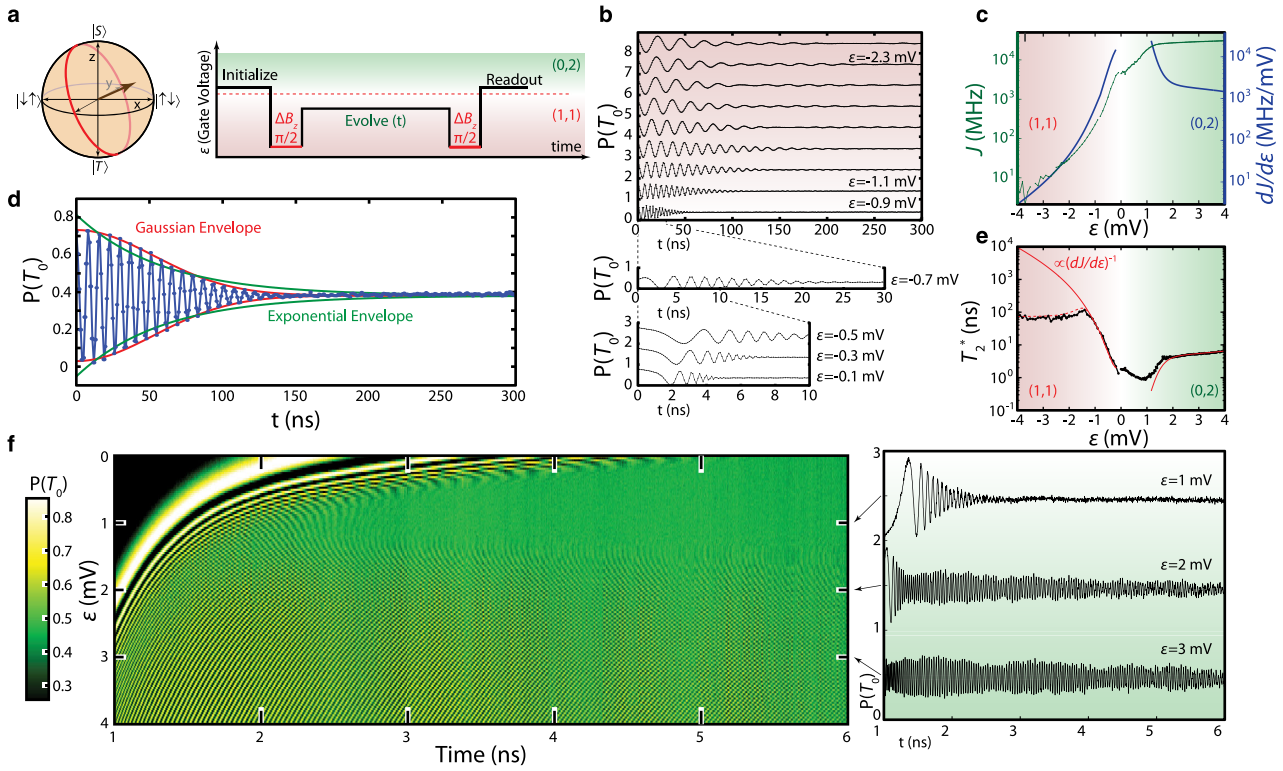

FIG. 2 (color online). Ramsey oscillations reveal low-frequency environmental dynamics. (a) The pulse sequence used to measure exchange oscillations uses a stabilized nuclear gradient to prepare and read out the qubit and has good contrast over a wide range of J. (b) Exchange oscillations consistently show larger T_2^* as J, and hence $dJ/d\epsilon$, shrinks until dephasing due to nuclear fluctuations sets in at very negative ϵ. (c) Extracted values of J and $dJ/d\epsilon$ as a function of ϵ. (d) The decay curve of FID exchange oscillations shows Gaussian decay. (e) Extracted values of T_2^* and $dJ/d\epsilon$. T_2^* is proportional to $(dJ/d\epsilon)^{-1}$, indicating that voltage noise causes the dephasing. (f) Exchange oscillations measured in (0, 2), showing slow dephasing at very positive ϵ. Line cuts at different values of ϵ show beats between the frequency of the oscillations and the sampling frequency.

making the (0, 2) $|S\rangle$ and (0, 2) $|T_0\rangle$ states electrostatically virtually identical. Here, as ϵ is increased, J increases but $dJ/d\epsilon$ decreases [Fig. 1(d)], allowing us to probe high quality exchange rotations and test our charge noise model in a regime that has never before been explored.

Using a modified pulse sequence that changes the clock frequency of our waveform generators to achieve a picosecond timing resolution (Fig. S1), we measure exchange oscillations in (0, 2) as a function of ϵ and time [Fig. 2(e)] and we extract both J [Fig. 2(c)] and T_2^* [Fig. 2(d)] as a function of ϵ. Indeed, the predicted behavior is observed: For moderate ϵ, we see fast oscillations that decay after a few ns, and for the largest ϵ we see even faster oscillations that decay slowly. Here, too, we observe that $T_2^* \propto (\frac{dJ}{d\epsilon})^{-1}$ [Fig. 2(d)], which indicates that the FID oscillations in (0, 2) are also primarily dephased by low-frequency voltage noise. We note, however, that we extract a different constant of proportionality between T_2^* and $(dJ/d\epsilon)^{-1}$ for (1, 1) and (0, 2). This is expected, given that the charge distributions associated with the qubit states are very different in these regimes and thus have different sensitivities to applied electric fields. We note that, in the regions of largest $dJ/d\epsilon$ (near $\epsilon = 0$), T_2^* is shorter than the rise time of our signal generator and we systematically underestimate J and overestimate T_2^* (Fig. S1). Accordingly, we omit $dJ/d\epsilon$ from Fig. 2(e)) in the regions where the data are untrustworthy (see the Supplemental Material [31]).

The above measurements indicate that the dephasing during FID experiments in both (1, 1) and (0, 2) arises overwhelmingly due to low-frequency (non-Markovian) noise, and the observed linear dependence of T_2^* on $(dJ/d\epsilon)^{-1}$ strongly suggests that ϵ noise is indeed responsible for the observed dephasing, as these data rule out dephasing from other mechanisms in most realistic situations (see the Supplemental Material [31], Sec. 5). In the presence of such low-frequency noise, the addition of a π pulse halfway through the free evolution can partially decouple the qubit from its noisy environment. Such a "Hahn-echo" [33] sequence prolongs coherence, which is useful for complex quantum operations [18], sensitive detection [34], and probing higher-frequency portions of the voltage noise bath. Rather than being sensitive to noise from dc to $1/\tau$ where τ is the total evolution time, these echo sequences have a noise sensitivity peaked at $f \approx 1/\tau$ and a reduced sensitivity at lower frequencies.

In our echo measurements, we select a fixed ϵ inside (1, 1) for free evolution and we sweep the length of the evolution following the π pulse by small increments δt to reveal an echo envelope [Figs. 3(a) and 3(b)]. The maximum amplitude of this observed envelope reveals the extent to which the state has dephased, while the Gaussian shape and width of the envelope arise from an effective single-qubit rotation for a time δt and reflect the same T_2^*. We note that this exchange echo is distinct from the echo measurements previously performed in singlet-triplet qubits [19–21] in that we use ΔB_z rotations to echo away voltage noise rather than J rotations to echo away noise in the nuclear bath.

The Hahn echo dramatically improves coherence times, with T_2^{echo} (the τ at which the observed echo amplitude has decayed by $1/e$) as large as 9 μs, corresponding to qualities ($Q \equiv T_2^{\text{echo}} J/2\pi$) larger than 600 [Fig. 3(c)]. If at high frequencies (50 kHz–1 MHz) the voltage noise were white (Markovian), we would observe exponential decay of the echo amplitude with τ. However, we find nonexponential decay [Fig. 3(d)], indicating that, even in the high-frequency band being probed by this measurement, the noise bath is non-Markovian.

A simple noise model that can account for this decay includes a mixture of white and $1/f$ noise

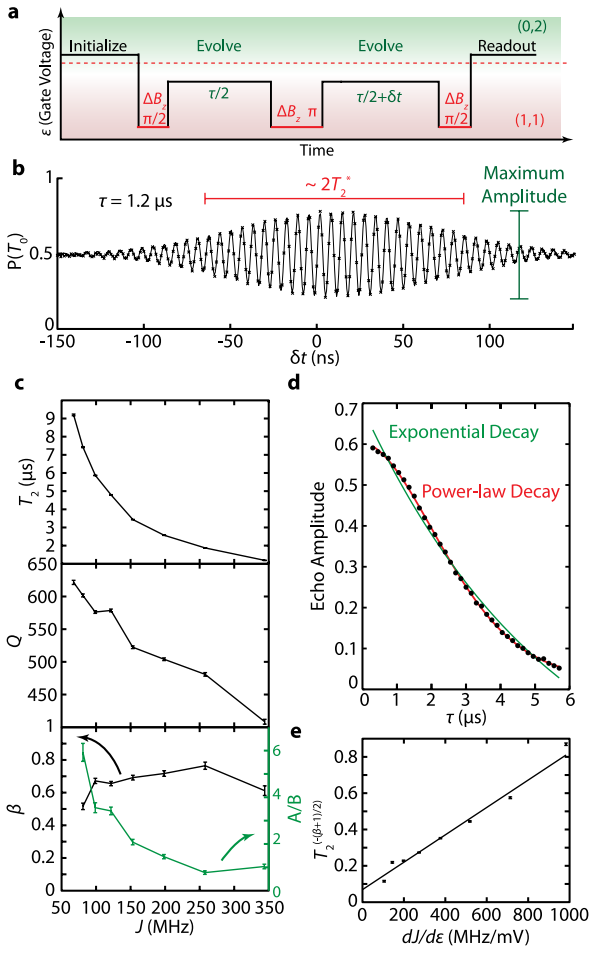

FIG. 3 (color online). Spin-echo measurements reveal high-frequency bath dynamics. (a) The pulse sequence used to measure exchange echo rotations. (b) A typical echo signal. The overall shape of the envelope reflects T_2^*, while the amplitude of the envelope as a function of τ (not pictured) reflects T_2^{echo}. (c) T_2^{echo} and $Q \equiv JT_2^{\text{echo}}/2\pi$ as a function of J. A comparison of the two noise models: Noise with a power-law spectrum fits over a wide range of ϵ (constant β), but the apparent relative contributions of white and $1/f$ noise change. (d) A typical echo decay is nonexponential but is well fit by $\exp[-(\tau/T_2^{\text{echo}})^{\beta+1}]$. (e) T_2^{echo} varies with $dJ/d\epsilon$ in a fashion consistent with dephasing due to power-law voltage fluctuations.

$S_\epsilon(f) = A + B/f$, which leads to an echo amplitude decay $\exp(-\tau/C_0 - \tau^2/C_1)$ [32], where $C_{0,1}$ are functions of the noise power. Since $C_{0,1}$ are both proportional to $(dJ/d\epsilon)^{-2}$, we expect the ratio $C_0/C_1 \propto A/B$ to be independent of $dJ/d\epsilon$. While this decay accurately describes the decay for a single value of ϵ, as we change ϵ (and therefore $dJ/d\epsilon$), we find that the ratio of white to $1/f$ noise power A/B changes, indicating that this model is inconsistent with our data [Fig. 3(c)]. Alternatively, we consider a power-law noise model $S_\epsilon(f) = \frac{S_0}{f^\beta}$, which leads to an echo amplitude decay $\exp[-(\tau/T_2^{\text{echo}})^{\beta+1}]$, with $T_2^{\text{echo}} \propto S_0^{-1/(\beta+1)}$. With this model, we expect β to be independent of $dJ/d\epsilon$ and we indeed observe $\beta \approx 0.7$ for all values of ϵ [Fig. 3(c)], indicating that this model can adequately describe our observed noise from approximately 50 kHz to 1 MHz. We further confirm that the observed dephasing is consistent with voltage noise by checking that T_2^{echo} has the expected dependence on $dJ/d\epsilon$, namely, $T_2^{\text{echo}} \propto (dJ/d\epsilon)^{-2/(\beta+1)}$ [Fig. 3(e)]. From the scale factor, we deduce that the noise is well approximated by $S_\epsilon(f) = 8 \times 10^{-16} \frac{\text{V}^2}{\text{Hz}} (\frac{1\ \text{Hz}}{f})^{0.7}$ from approximately 50 kHz to 1 MHz, corresponding to ϵ noise of $0.2\ \text{nV}/\sqrt{\text{Hz}}$ at 1 MHz. This noise exceeds that accounted for by known sources of noise present in the experiment, including instrumental noise on the device gates and Johnson noise of the wiring. The rms noise deduced from our FID measurements exceeds that expected from this power-law noise; there is excess noise at very low frequencies in the device.

Thus far, we have explored the voltage noise bath at the base temperature of our dilution refrigerator ($\mathcal{T} \approx 50\,\text{mK}$). We gain additional insight into the properties of the voltage noise by studying its temperature dependence. We observe no $\mathcal{T}$ dependence of the dephasing time $T^*_{2,\text{nuclear}}$ for ΔB_z rotations [Fig. 4(a)], which is expected since since 50 mk is much larger than the nuclear Zeeman splitting.

By contrast, T_2^* due to exchange oscillations in (1, 1) and (0, 2) show unexpected temperature dependences [Fig. 4(b)]. These have the same scaled temperature dependence $T^*_{2,(1,1)}(\mathcal{T}) \propto T^*_{2,(0,2)}(\mathcal{T})$, suggesting that the loss of coherence is due to the same mechanism, presumably increased voltage noise, in both instances. In both cases, T_2^* is roughly linear with $\mathcal{T}$, indicating that only small gains are likely to be made in the quality of FID-based rotations by reducing $\mathcal{T}$. By comparison, T_2^{echo} shows a strong dependence of $T_2^{\text{echo}} \propto \mathcal{T}^{-2}$ [Fig. 4(c)]. As $\mathcal{T}$ is increased, the observed noise becomes increasingly frequency independent [Fig. 4(d)], although measurements of β become inaccurate at large $\mathcal{T}$ where T_2^{echo} is small. We note that the underlying mechanism of this temperature dependence is currently unknown; however, the dependence of the observed dephasing on temperature strongly suggests that the noise originates within the device rather than the experimental apparatus. Lower temperatures carry a double benefit for echo coherence; the noise becomes both smaller and more non-Markovian, thereby increasing coherence times and extending the potential for multipulse dynamical decoupling sequences to mitigate the effects of the noise [35,36]. This trend shows no indication of saturating at low temperatures; it appears likely that much longer coherence times are attainable by reducing temperatures with more effective refrigeration (Fig. S3).

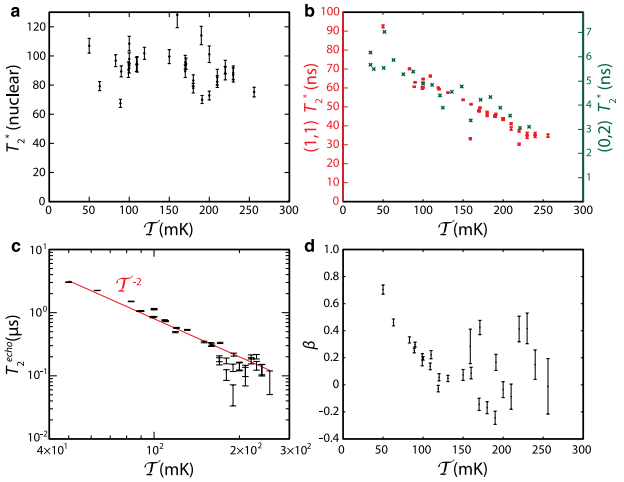

FIG. 4 (color online). Higher temperatures speed dephasing. (a) $T^*_{2,\text{nuclear}}$ does not depend significantly on $\mathcal{T}$. (b) T_2^* in (1, 1) (red squares) and (0, 2) (green crosses) has the same weak, scaled dependence on $\mathcal{T}$. (c) T_2^{echo} shows a strong temperature dependence near $\mathcal{T}^{-2}$ (red line) across over an order of magnitude in coherence times. (d) As $\mathcal{T}$ is increased, β approaches zero, indicating that the noise leading to decoherence becomes nearly white. Uncertainties in β are larger at higher temperatures due to the fast decay of the echo.

Operating at base temperature and using the Hahn-echo sequence described above, we observe a voltage sensitivity of $0.2\ \text{nV}/\sqrt{\text{Hz}}$ at 1 MHz, which suggests that the qubit can be used as a sensitive electrometer at this frequency. In order to compare to other electrometers, we convert our voltage sensitivity into a charge sensitivity of $2 \times 10^{-8} e/\sqrt{\text{Hz}}$ by dividing by the Coulomb blockade peak spacing 10 mV. This value is nearly 2 orders of magnitude better than the theoretical limits for rf single electron transistors [37] and is limited only by T_2^{echo}, which the data suggest can be improved.

Using both FID and echo measurements, we have characterized the exchange interaction and presented experimental evidence that exchange rotations in S-T_0 qubits dephase due to voltage noise. These measurements reveal that the voltage noise bath that couples to the qubit is non-Markovian and establish baseline noise levels for S-T_0 qubits. We suggest that further improvements in operation fidelity and charge sensitivity are possible by reducing $\mathcal{T}$, using more complex pulse sequences such as Carr-Purcell-Meiboom-Gill [35] and Uhrig dynamical decoupling [36], and performing operations at larger J ($dJ/d\epsilon$) to move to a higher-frequency portion of the noise spectrum with potentially lower noise. In particular, because two-qubit

operations in S-T_0 qubits rely on exchange echo [18], our data show a path forward for increasing two-qubit gate fidelities in these devices.

This work is supported through the ARO, Precision Quantum Control and Error-Suppressing Quantum Firmware for Robust Quantum Computing. This research was funded by the Office of the Director of National Intelligence (ODNI), Intelligence Advanced Research Projects Activity (IARPA), through the Army Research Office Grant No. W911NF-11-1-0068. All statements of fact, opinion or conclusions contained herein are those of the authors and should not be construed as representing the official views or policies of IARPA, the ODNI, or the U.S. Government. This work is sponsored by the United States Department of Defense. The views and conclusions contained in the document are those of the authors and should not be interpreted as representing the official policies, either expressly or implied, of the U.S. Government. This work was performed in part at the Center for Nanoscale Systems (CNS), a member of the National Nanotechnology Infrastructure Network (NNIN), which is supported by the National Science Foundation under NSF Grant No. ECS-0335765. CNS is part of Harvard University. O. E. D. and M. D. S. contributed equally to this work.

*Present address: 2nd Institute of Physics C, RWTH Aachen University, 52074 Aachen, Germany.

[1] D. DiVincenzo, Fortschr. Phys. **48**, 771 (2000).
[2] B. M. Chernobrod and G. P. Berman, J. Appl. Phys. **97**, 014903 (2005).
[3] P. Maletinsky, S. Hong, M. S. Grinolds, B. Hausmann, M. D. Lukin, R. L. Walsworth, M. Loncar, and A. Yacoby, Nat. Nanotechnol. **7**, 320 (2012).
[4] R. Hanson, L. P. Kouwenhoven, J. R. Petta, S. Tarucha, and L. M. K. Vandersypen, Rev. Mod. Phys. **79**, 1217 (2007).
[5] D. Loss and D. P. DiVincenzo, Phys. Rev. A **57**, 120 (1998).
[6] J. Levy, Phys. Rev. Lett. **89**, 147902 (2002).
[7] J. M. Taylor, H.-A. Engel, W. Dür, A. Yacoby, C. M. Marcus, P. Zoller, and M. D. Lukin, Nat. Phys. **1**, 177 (2005).
[8] F. H. L. Koppens, C. Buizert, K. J. Tielrooij, I. T. Vink, K. C. Nowack, T. Meunier, L. P. Kouwenhoven, and L. M. K. Vandersypen, Nature (London) **442**, 766 (2006).
[9] D. J. Reilly, C. M. Marcus, M. P. Hanson, and A. C. Gossard, Appl. Phys. Lett. **91**, 162101 (2007).
[10] K. C. Nowack, F. H. L. Koppens, Y. V. Nazarov, and L. M. K. Vandersypen, Science **318**, 1430 (2007).
[11] M. Pioro-Ladrière, Y. Tokura, T. Obata, T. Kubo, and S. Tarucha, Appl. Phys. Lett. **90**, 024105 (2007).
[12] J. M. Taylor, J. R. Petta, A. C. Johnson, A. Yacoby, C. M. Marcus, and M. D. Lukin, Phys. Rev. B **76**, 035315 (2007).
[13] M. Pioro-Ladriere, T. Obata, Y. Tokura, Y. S. Shin, T. Kubo, K. Yoshida, T. Taniyama, and S. Tarucha, Nat. Phys. **4**, 776 (2008).
[14] C. Barthel, D. J. Reilly, C. M. Marcus, M. P. Hanson, and A. C. Gossard, Phys. Rev. Lett. **103**, 160503 (2009).
[15] H. O. H. Churchill, F. Kuemmeth, J. W. Harlow, A. J. Bestwick, E. I. Rashba, K. Flensberg, C. H. Stwertka, T. Taychatanapat, S. K. Watson, and C. M. Marcus, Phys. Rev. Lett. **102**, 166802 (2009).
[16] S. Foletti, H. Bluhm, D. Mahalu, V. Umansky, and A. Yacoby, Nat. Phys. **5**, 903 (2009).
[17] S. Nadj-Perge, S. M. Frolov, E. P. A. M. Bakkers, and L. P. Kouwenhoven, Nature (London) **468**, 1084 (2010).
[18] M. D. Shulman, O. E. Dial, S. P. Harvey, H. Bluhm, V. Umansky, and A. Yacoby, Science **336**, 202 (2012).
[19] H. Bluhm, S. Foletti, I. Neder, M. S. Rudner, D. Mahalu, V. Umansky, and A. Yacoby, Nat. Phys. **7**, 109 (2011).
[20] C. Barthel, J. Medford, C. M. Marcus, M. P. Hanson, and A. C. Gossard, Phys. Rev. Lett. **105**, 266808 (2010).
[21] J. Medford, L. Cywiński, C. Barthel, C. M. Marcus, M. P. Hanson, and A. C. Gossard, Phys. Rev. Lett. **108**, 086802 (2012).
[22] J. R. Petta, A. C. Johnson, J. M. Taylor, E. A. Laird, A. Yacoby, M. D. Lukin, C. M. Marcus, M. P. Hanson, and A. C. Gossard, Science **309**, 2180 (2005).
[23] I. van Weperen, B. D. Armstrong, E. A. Laird, J. Medford, C. M. Marcus, M. P. Hanson, and A. C. Gossard, Phys. Rev. Lett. **107**, 030506 (2011).
[24] R. Brunner, Y.-S. Shin, T. Obata, M. Pioro-Ladrière, T. Kubo, K. Yoshida, T. Taniyama, Y. Tokura, and S. Tarucha, Phys. Rev. Lett. **107**, 146801 (2011).
[25] K. C. Nowack, M. Shafiei, M. Laforest, G. E. D. K. Prawiroatmodjo, L. R. Schreiber, C. Reichl, W. Wegscheider, and L. M. K. Vandersypen, Science **333**, 1269 (2011).
[26] E. A. Laird, J. M. Taylor, D. P. DiVincenzo, C. M. Marcus, M. P. Hanson, and A. C. Gossard, Phys. Rev. B **82**, 075403 (2010).
[27] L. Gaudreau, G. Granger, A. Kam, G. C. Aers, S. A. Studenikin, P. Zawadzki, M. Pioro-Ladrière, Z. R. Wasilewski, and A. S. Sachrajda, Nat. Phys. **8**, 54 (2011).
[28] D. Culcer, X. Hu, and S. Das Sarma, Appl. Phys. Lett. **95**, 073102 (2009).
[29] B. M. Maune, M. G. Borselli, B. Huang, T. D. Ladd, P. W. Deelman, K. S. Holabird, A. A. Kiselev, I. Alvarado-Rodriguez, R. S. Ross, A. E. Schmitz, M. Sokolich, C. A. Watson, M. F. Gyure, and A. T. Hunter, Nature (London) **481**, 344 (2011).
[30] H. Bluhm, S. Foletti, D. Mahalu, V. Umansky, and A. Yacoby, Phys. Rev. Lett. **105**, 216803 (2010).
[31] See Supplemental Material at http://link.aps.org/supplemental/10.1103/PhysRevLett.110.146804 for details about the pulse sequences used to measure the exchange splitting, the fitting procedures, and the formulas for extracting noise power. It also contains brief notes on the temperature dependent noise, the relaxation time (T1) of the qubit, and the contribution to dephasing from other parameters.
[32] L. Cywinski, R. M. Lutchyn, C. P. Nave, and S. Das Sarma, Phys. Rev. B **77**, 174509 (2008).
[33] E. L. Hahn, Phys. Rev. **80**, 580 (1950).
[34] J. R. Maze, P. L. Stanwix, J. S. Hodges, S. Hong, J. M. Taylor, P. Cappellaro, L. Jiang, M. V. Gurudev Dutt, E. Togan, A. S. Zibrov, A. Yacoby, R. L. Walsworth, and M. D. Lukin, Nature (London) **455**, 644 (2008).
[35] H. Y. Carr and E. M. Purcell, Phys. Rev. **94**, 630 (1954).
[36] G. S. Uhrig, Phys. Rev. Lett. **98**, 100504 (2007).
[37] M. H. Devoret and R. J. Schoelkopf, Nature (London) **406**, 1039 (2000).